ESC European Society of Cardiology

European Heart Journal Open (2023) **3**, 1–9
https://doi.org/10.1093/ehjopen/oead099

ORIGINAL ARTICLE
Translational basic science

Instantaneous detection of acute myocardial infarction and ischaemia from a single carotid pressure waveform in rats

Rashid Alavi [1], Wangde Dai[2,3], Ray V. Matthews[2,4], Robert A. Kloner[2,3,*], and Niema M. Pahlevan [1,2,3,*]

[1]Department of Aerospace and Mechanical Engineering, University of Southern California, 3650 McClintock Ave. Room 400, Los Angeles, CA 90089, USA; [2]Division of Cardiovascular Medicine, Keck School of Medicine, University of Southern California, 1975 Zonal Ave., Los Angeles, CA 90033, USA; [3]Cardiovascular Research Institute, Huntington Medical Research Institutes, 686 S Fair Oaks Ave., Pasadena, CA 91105, USA ; and [4]Cardiac and Vascular Institute, University of Southern California, 1975 Zonal Ave., Los Angeles, CA 90033, USA

Received 13 April 2023; revised 17 August 2023; accepted 25 September 2023; online publish-ahead-of-print 3 October 2023

Handling Editor: Daniel F.J. Ketelhuth

Aims

Myocardial infarction (MI) is one of the leading causes of death worldwide. It is well accepted that early diagnosis followed by early reperfusion therapy significantly increases the MI survival. Diagnosis of acute MI is traditionally based on the presence of chest pain and electrocardiogram (ECG) criteria. However, around 50% of the MIs are without chest pain, and ECG is neither completely specific nor definitive. Therefore, there is an unmet need for methods that allow detection of acute MI or ischaemia without using ECG. Our hypothesis is that a hybrid physics-based machine learning (ML) method can detect the occurrence of acute MI or ischaemia from a single carotid pressure waveform.

Methods and results

We used a standard occlusion/reperfusion rat model. Physics-based ML classifiers were developed using intrinsic frequency parameters extracted from carotid pressure waveforms. ML models were trained, validated, and generalized using data from 32 rats. The final ML models were tested on an external stratified blind dataset from additional 13 rats. When tested on blind data, the best ML model showed specificity = 0.92 and sensitivity = 0.92 for detecting acute MI. The best model's specificity and sensitivity for ischaemia detection were 0.85 and 0.92, respectively.

Conclusion

We demonstrated that a hybrid physics-based ML approach can detect the occurrence of acute MI and ischaemia from carotid pressure waveform in rats. Since carotid pressure waveforms can be measured non-invasively, this proof-of-concept pre-clinical study can potentially be expanded in future studies for non-invasive detection of MI or myocardial ischaemia.

* Corresponding author. Tel: +1 626 389 3413, Email: robert.kloner@hmri.org; Tel: +1 (213) 740 7182, Email: pahlevan@usc.edu

Graphical Abstract

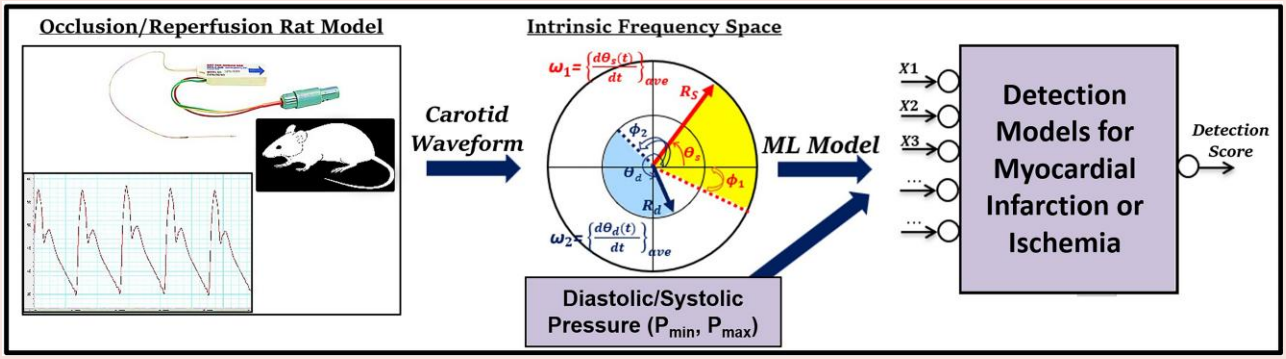

Keywords Acute myocardial infarction/ischaemia • Diagnosis • Arterial waveform • Cardiovascular intrinsic frequency • Machine learning

Introduction

Myocardial infarction (MI), necrosis of heart muscle secondary to prolonged lack of oxygen supply (myocardial ischaemia), is one of the leading causes of death worldwide. Each year, an estimated 8.5 million cases of acute MI happen worldwide,[1] with high mortality rates of up to 10% after a month and 25% after a year.[2] Potential MI patients are usually rushed to the hospital after experiencing severe chest pain, in order to receive reperfusion therapy (stenting or more rarely thrombolytic therapy). There is also a direct relationship between mortality and the extent of MI, and duration of coronary occlusion,[3] so early diagnosis, reperfusion, and therapy[4] lead to increased survival. The time an acute MI patient spends at home contemplating symptoms is also important to be minimized especially considering that almost 50% of all MIs happen without chest pain (silent MI)[1] or with pain not typical of MI or that the MI manifests as other symptoms rather than classical chest pain. The electrocardiogram (ECG) is generally considered to be the principal non-invasive test for the diagnosis of acute MI,[5] but it is neither specific nor definitive[6] when used alone and requires expert interpretation. The ECG can be non-specific for the first 4–8 h in MI patients[7]; however, 50% of the patients succumb from MI within the first 45–60 min after the symptoms onset,[7,8] showing the significance of early diagnostics. In addition, it has been shown that 43% of 281 MI patients (confirmed by autopsy) had non-diagnostic ECGs.[9] Therefore, there is an unmet need for instantaneous, inexpensive, and non-invasive methods for detection of MI and ischaemia that do not use ECG.

A sudden decrease in left ventricle (LV) contractile performance and an increase in LV filling pressure are among the first haemodynamic abnormalities that occur within seconds of coronary artery occlusion.[10,11] These are followed by various regulatory responses that affect vascular function and LV-arterial coupling.[12] Our general hypothesis recently was that a system approach such as intrinsic frequency (IF) method combined with machine learning (ML) algorithms can detect signatures of pathophysiology associated with different cardiovascular diseases (e.g. in this study, acute MI or myocardial ischaemia) from carotid pressure waveforms. The IF method[13–15] is an integrative systems approach that considers the LV and arterial network as a coupled dynamical system (LV + arterial tree) during systole which becomes decoupled during diastole (upon closure of the aortic valve). Several clinical studies have recently demonstrated that the IF method reveals clinically relevant information about LV function, vascular dynamics, and LV-arterial coupling. In a blind clinical study of a heterogeneous adult cohort ($n = 72$), Pahlevan *et al.*[15] demonstrated that LV ejection fraction (LVEF) can be evaluated by applying the IF method on carotid waveforms measured by a smartphone (an iPhone).[15] In their study, the LVEF derived from IF-iPhone had a strong correlation ($r = 0.94$) with LVEF measured by cardiac magnetic resonance (CMR) imaging in heart failure (HF) patients. In a cohort of childhood cancer survivors ($n = 191$), it was demonstrated that LVEF derived from carotid pressure waveforms measured by a portable hand-held device is more accurate than a two-dimensional echocardiogram when compared with the gold standard CMR.[16] In a recent study, Cooper *et al.* used the longitudinally followed large cohort of the Framingham Heart Study (FHS)[14] and demonstrated that IFs of carotid pressure waveforms are associated with higher risks for incidents of HF and composite cardiovascular disease (CVD) events, independent from other cardiovascular risk factors.[17] Using the Framingham (FHS) data, it was also shown that aortic stiffness (as measured by carotid-femoral pulse wave velocity) can be computed using a hybrid IF-ML methodology applied on a single non-invasively measured carotid pressure waveform (without the need for ECG or femoral tonometry).[17] In a recent invasive clinical study, Mogadam *et al.*[18] demonstrated the efficacy and robustness of the IF method for instantaneous assessment of LV-arterial coupling after transcatheter aortic valve replacement. These clinical studies point to (i) the importance of the IF method for non-invasive evaluation of LV arterial function and (ii) the suitability of IF method for ML algorithms.

Our goal in this study is to provide the proof-of-concept that the hybrid IF-ML approach (a physics-based ML approach) can be expanded for detection of acute MI or myocardial ischaemia (brief ischaemia without infarction) from a single carotid waveform in rats. We adopted different ML classifiers, e.g. random forest (RF) or support vector (SV) classifiers to ensure our approach is independent of ML algorithm. To ensure that our developed models were not simply distinguishing the baseline from any abnormal event, we tested the MI detection models using ischaemia data (which represents a different abnormal event). This test was performed to confirm that our models did not just detect post-occlusion abnormalities. This was further evidenced by the fact that the MI detection models' predictions were not sensitive to the myocardial ischaemia data points. Our IF-ML method uses carotid

pressure waveforms that can be measured non-invasively, and scalability of IF parameters between other mammals (rat and rabbit) and human has been shown.[13] Therefore, this proof-of-concept preclinical study offers potential for future research into the non-invasive detection of MI or myocardial ischaemia.

Methods

Standard rat model for acute myocardial infarction and ischaemia

In this study, we use a standard acute MI/ischaemia rat model {$n = 45$; Sprague–Dawley female rats; ~200 g body weight; age of 7 ± 1 weeks [mean ± standard deviation (SD)]}. Surgeries were performed on fully anaesthetized rats to impose myocardial ischaemia and infarction. Full anaesthesia was achieved using intra-peritoneal ketamine and xylazine based on animal's weight (intra-peritoneal ketamine 75 mg/kg body weight and xylazine 5 mg/kg). A neck incision was performed to isolate the carotid artery and jugular vein for catheter placement. Then, catheterization was conducted through the right carotid artery to reach the target locations in the arterial system and LV. Left thoracotomy was then performed to expose the heart (the chest cavity was opened through an incision in the 4th left intercostal). To expose the anterior surface of the LV, the pericardium was gently removed. The proximal left coronary artery was subsequently isolated followed by mechanical occlusion of the coronary artery for 30 min to ensure the infarction.[19,20] After the 30 min coronary occlusion, coronary artery reperfusion was performed for 3 h. More details about the techniques and steps of the surgery are provided in Supplementary material online, Supplement A.

The presence of MI was confirmed after the surgery through histopathology followed by measuring the size of infarction (i.e. mass percentage of necrosis over total LV). To achieve that, the four heart slices were incubated in 1% triphenyl tetrazolium chloride (TTC), a chemical that stains viable cells brick red, while dead or necrotic cells appear white to yellow. The range of infarct sizes in our study was calculated as $33.5 \pm 11.6\%$ (i.e. mean ± SD). More details regarding the measurement of MI size are provided in Supplementary material online, Supplement A.

It is worth mentioning that we have waited for at least 30 min after the start of the anaesthesia to resume the procedure. One main reason is to make sure that the temporary effects of anaesthesia on haemodynamics are finished, and therefore, the following haemodynamic changes are due to the cardiovascular events. The employed procedures in this study were approved by the Institutional Animal Care and Use Committees at Huntington Medical Research Institutes. All the surgical steps were conducted according to the guidelines for the care and use of laboratory animals (NIH publication No. 85-23, National Academy Press, Washington, DC, revised 2011).

Invasive haemodynamic measurements

General tracings and haemodynamics including carotid pressure, volume, ECG signal (29 gauge needle electrodes, 3 leads), and temperature were continuously measured, monitored, and recorded throughout the surgical operations (starting from after full anaesthesia to 3 h after reperfusion). Pressure waveforms were measured at the carotid artery using a 2F high-fidelity piezo-tipped micro-manometer (model SPR-869, Millar Mikro-Cath Pressure Catheter). Catheter calibration was conducted before each surgery. Body temperature was measured and monitored using a rectal thermocouple probe. The LabChart-Pro (ADInstruments, Ltd) is used as the platform software for our data measurements via PowerLab 4/35 data acquisition system (ADInstruments, Ltd).

Intrinsic frequency method

The IF method[13–15,21,22] is a systems approach considering the LV and arterial network as a coupled dynamical system (LV + arterial tree) during systole which becomes decoupled during diastole (after closure of the aortic valve). The IF frequencies are defined as operating frequencies based on the sparse time-frequency representation.[23] The mathematical formulation of the IF method is given by:

$$\begin{aligned}\text{Minimize: } \| p(t) - \chi(0, T_0)[a_1 \cos(\omega_1 t) + b_1 \sin(\omega_1 t)] \\ - \chi(T_0, T)[a_2 \cos(\omega_2 t) + b_2 \sin(\omega_2 t)] - c\|_2^2 \end{aligned} \quad (1)$$

Equation (1) can also be rewritten as:

$$\begin{aligned}\text{Minimize: } \| p(t) - \chi(0, T_0)[R_s \sin(\omega_1 t + \varphi_1)] \\ - \chi(T_0, T)[R_d \sin(\omega_2 t + \varphi_2)] - c\|_2^2 \end{aligned} \quad (2)$$

Where $p(t)$ refers to the arterial waveform (e.g. carotid, femoral, or aortic) and $\chi(a, b)$ refers to an indicator function defined by $\chi(\alpha, \beta) = 1$ if $\alpha \le t \le \beta$ and $\chi(\alpha, \beta) = 0$ otherwise. Here, ω_1 and ω_2 are the first and the second IFs, respectively (or systolic and diastolic IFs, respectively). T_0 denotes the time of LV-arterial decoupling when the aortic valve closure happens (the dicrotic notch time), and T refers to the cardiac cycle duration. The envelopes (R_s and R_d) and the initial intrinsic phases ($\varphi_1$and φ_2) of Equation (2) are defined in terms of a_1, b_1, a_2, and b_2 as $R_s = \sqrt{a_1^2 + b_1^2}$, $R_d = \sqrt{a_2^2 + b_2^2}$, $\varphi_1 = \tan^{-1}(a_1/b_1)$, and $\varphi_2 = \tan^{-1}(a_2/b_2)$ The parameters R_s and R_d are the envelopes of the systolic and diastolic IFs, respectively. φ_1 and φ_2 refer to the initial phase shifts (also called intrinsic phases) of the IF components associated with ω_1 and ω_2, respectively. Relative height of decoupling at the dicrotic notch (RHDN) is defined as the ratio of the height of the decoupling (relative to P_{min}) with respect to the total signal variation (P_{max}–P_{min}). Mathematical formulation of the IF method, its accuracy, its computational procedure, as well as its scalability among different mammalian species (rat, rabbit, human) and measurement modalities (piezoelectric tonometry, optical tonometry, smartphone camera) can be found in previous studies.[13–15,21,24]

From physiological point of view, the systolic IF parameters such as ω_1, φ_1, and R_s are mainly defined by the contractile performance of LV and the dynamics of the coupled LV-arterial system.[15,21] On the other hand, the diastolic IF parameters such as ω_2, φ_2, and R_d are dominated by the vascular function and arterial dynamics.[17,21,25–28] Since R_s and R_d values require calibration, we considered the non-dimensional ratio R_s/R_d that is defined as the envelope ratio (ER).[21] Hence, ER depends on both LV and vascular function, and it does not require pressure calibration. *Figure 1A* shows a reconstruction of an arterial pulse waveform (here carotid waveform) using the IF method, and *Figure 1B* presents the physical representation of ω_1, ω_2, φ_1, φ_2, R_s, and R_d during the systolic and diastolic phases.

Physics-based feature selection for machine learning

The selection of input parameters for ML algorithm is one of the most important steps for a successful training and development of hybrid physics-informed ML models especially when limited data are available. ω_1, ω_2, φ_1, ER, and RHDN are selected based on their physiological relevancy as mentioned above.[15,21] Since these IF parameters do not need pressure calibration,[15] they are used for non-calibrated IF-ML model development. Systolic pressure of the carotid waveform (P_{max}) and carotid diastolic pressure (P_{min}) are added for calibrated IF-ML models. Other pressure metrics such as pulse pressure or mean pressure could have been used, but any of these can be approximated from P_{min} and P_{max} (no additional benefit from ML perspective). We considered all possible input set variations of (ω_1, ω_2, φ_1, ER, and RHDN) for uncalibrated IF-ML model development and all possible variations of (ω_1, ω_2, φ_1, ER, RHDN, P_{min}, P_{max}) for calibrated IF-ML models. The best input sets were selected based on the training and generalization performance of our ML.

For each rat, features are extracted from invasively measured carotid pressure waveforms at three different time points: 5 min before coronary occlusion (baseline healthy), 5 min after occlusion (ischaemia without infarction),[29] and 2 h after reperfusion of the 30 min occlusion (acute MI).[19,20] At each time point, the beginning, the dicrotic notch, and the end of a randomly selected cycle are manually identified for features calculations.

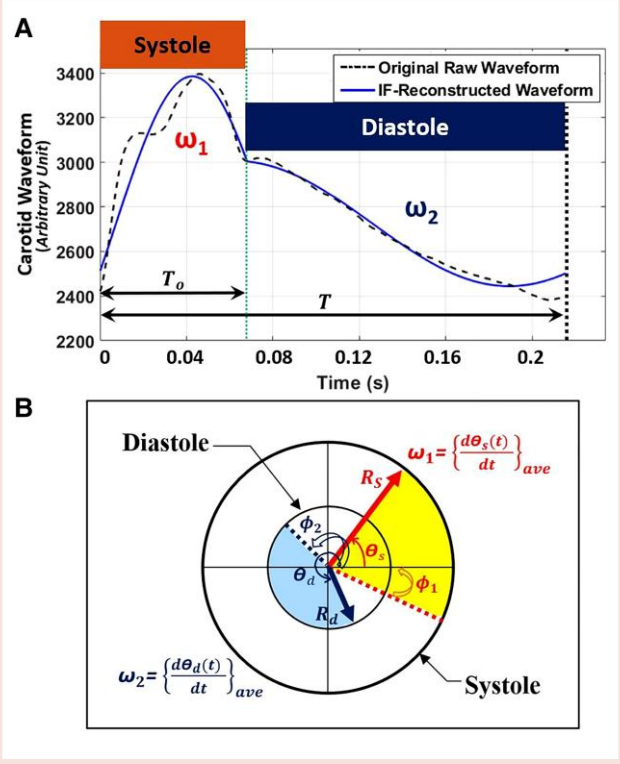

Figure 1 Visualization of the basics of the intrinsic frequency method. (*A*) An intrinsic frequency-reconstructed carotid waveform (solid blue) overlaid on the original raw waveform in arbitrary units (dashed black). (*B*) Intrinsic frequency visualization during a full cardiac cycle. The parameters ω_1 and ω_2 are intrinsic frequencies during systole and diastole, respectively. $d\theta/dt$ represents the instantaneous frequency,[21] and the parameters R_s and R_d are the envelopes of the intrinsic frequency reconstruction corresponding to ω_1 and ω_2, respectively (in general, $R_s \neq R_d$). The parameters φ_1 and φ_2 are the initial intrinsic phases corresponding to ω_1 and ω_2, respectively.

Machine learning procedure and evaluation

Different classifier algorithms, i.e. RF classifier (RFC) and SV classifier (SVC) as well as two more ML algorithms (see Supplementary material online, Supplement *I*), were employed to ensure the independency of our method from any specific ML algorithm. We adopted the k-fold cross-validation (CV) method as well as the blind test (so-called 'external validation') and 95% confidence interval analysis using bootstrap resampling in order to validate our ML models against any possible overfitting. All the input set variations that were possible based on the physiological features (see above) were used for training the classifiers (the best input sets will be determined later based on performance of the classifiers). The model outputs were defined as binary classifications of waveforms by model output = {no ischaemia; ischaemia} or model output = {no MI; MI} for detection of acute ischaemia and acute MI, respectively. The hyper-parameters that were optimized in the training/validation process for RFCs included the split criterion [i.e. {gini, entropy}], maximum depth [i.e. {4, 5, 7, 8, 10, 12, 20}]; max-features [i.e. {sqrt, log2}], and number of estimators [i.e. {5, 7, 10, 15, 20, 25, 30, 40, 50}]. For the SVCs, the hyper-parameters included Kernel function [i.e. {linear, rbf, sigmoid}] and Kernel coefficient [i.e. {scale, auto}].

The design process of our ML models was evaluated by multiple parameters such as training score, CV average score, generalization test results (specificity, sensitivity, and accuracy), and the area under the curve (AUC) defined by receiver operating characteristic (ROC). Sensitivity, specificity, and accuracy are defined as:

$$\text{Sensitivity} = (\text{true positive})/(\text{true positive} + \text{false negative}),$$

$$\text{Specificity} = (\text{true negative})/(\text{true negative} + \text{false positive}),$$

$$\text{Accuracy} = (\text{true positive} + \text{true negative})/(\text{all positive} + \text{all negative})$$

Our accuracy threshold criteria for accepting accurate classifiers in the training level are described in Supplementary material online, Supplement *B*. Evaluation metrics for blind (external) test are sensitivity, specificity, and AUC.

More details about the procedure of our physics-based hybrid IF-ML approach are presented in Supplementary material online, Supplement *C*, where the flowchart diagram of the method is also presented (see Supplementary material online, Figure S2). All the ML models were trained and evaluated implementing Keras with TensorFlow Core v.2.8.0 as the backend.[30] Further details about the RFC and SVC algorithms can be found in Supplementary material online, Supplement *D*.

Data specifications for training, generalization, and blind test

In this study, $n = 45$ rats are used, so there are $n = 45$ waveforms for normal baseline condition, $n = 45$ waveforms for acute myocardial ischaemia (brief ischaemia without infarction), and $n = 45$ waveforms for acute MI (the total number $n = 135$ waveforms). We applied the stratified blind test technique (or a so-called 'external validation') by putting aside 30% of the rats (i.e. 13 rats or 39 waveforms) for the blind test prior to the parameter selection and ML procedure. Setting 30% as external validation would meet minimal sample size requirements for diagnostic accuracy analysis in a 2×2 confusion matrix with only two true cells. The blind dataset was kept blind to all the stages of the feature selections and model design. The remaining 70% (i.e. 32 rats or 96 waveforms) were employed for the design process of the ML classifier models. We further divided this design data into 80% for training and 20% for generalization test. The same ML design procedure and blind test rats were used for both myocardial ischaemia and acute MI detections. After data specifications, the distribution of infarct sizes stayed comparable between the ML design rats (34.7% ± 11.6%, i.e. mean ± SD) and the blind rats (30.3% ± 10.2%, i.e. mean ± SD).

Results

Table 1 presents statistics (mean value ± SD) of the baseline haemodynamics and IF parameters corresponding to all rats, the ML design rats (used for ML model training and generalization), and the blind test rats (which were kept blind to all the stages of the ML model development). The two-sample student's *t*-test was applied to confirm the similarity in the baseline haemodynamics and IF parameters between the ML design rats and the blind test rats. The results showed *P* values of $P = 0.79$ (heart rate), $P = 0.83$ (P_{min}), $P = 0.98$ (P_{max}), $P = 0.26$ (ω_1), $P = 0.52$ (ω_2), $P = 0.41$ (ϕ_1), $P = 0.98$ (ER), and $P = 0.72$ (RHDN). Since $P > 0.05$ was achieved for all the parameters, no significant differences were observed.

Machine learning-based detection models for acute myocardial infarction

The best optimal classifiers for acute MI detection (for both RFC and SVC) were chosen based on our accuracy threshold criteria (see Supplementary material online, Supplement *B*) for both uncalibrated and calibrated input vectors. The characteristics/accuracy summary of the selected models from both classifier algorithms is presented in *Table 2*. As shown in *Table 2*, the input vectors {ω_1, φ_1, ER} and {ω_1, φ_1, ER, P_{min}} are the best sets that are selected by each classifier algorithm (RF and SVC). Here, 'All Tests' includes all blind test rats plus

Table 1 Baseline haemodynamics and intrinsic frequency parameters for all rats, machine learning design rats, and blind test rats

Parameter	All rats	ML design rats	Blind test rats
Number, *n* (%)	45 (100%)	32 (70%)	13 (30%)
Heart rate (b.p.m.)	278 ± 25	277 ± 26	281 ± 25
P_{min} (mmHg)	65.6 ± 10.4	65.8 ± 10.8	65.1 ± 9.6
P_{max} (mmHg)	91.8 ± 11.1	91.7 ± 11.7	92.1 ± 10.0
ω_1 (b.p.m.)	422.9 ± 31.7	419.4 ± 35.6	431.5 ± 17.0
ω_2 (b.p.m.)	299.6 ± 75.7	293.4 ± 73.4	314.8 ± 82.1
φ_1 (radian)	−0.32 ± 0.12	−0.33 ± 0.13	−0.29 ± 0.08
ER	3.14 ± 0.76	3.13 ± 0.83	3.15 ± 0.54
RHDN	0.45 ± 0.17	0.45 ± 0.19	0.43 ± 0.14

Values are presented in mean value ± SD.
ω_1, first intrinsic frequency; ω_2, second intrinsic frequency; φ_1, first initial intrinsic phase; ER, envelope ratio; RHDN, relative height of decoupling at the dicrotic notch.

rats that were used for testing during ML model development. 'All Data' includes all 45 rats used in this study (blind test rats + ML design rats). ROC curves of the selected models for acute MI detection are shown in *Figure 2*. Details about the optimal hyper-parameters of each classifier and the confusion matrices of the selected models are provided in Supplementary material online, Supplement *E* (Supplementary material online, *Table S1*) and Supplement *F* (see Supplementary material online, Figure *S3*), respectively.

When tested on blind (external) data, the uncalibrated model from the SVC algorithm outperformed the model from RF in terms of specificity. However, when considering the AUC metric, the overall performance of the RF model was slightly superior to that of the SVC (*Figure 2*). Notably, the performance of the models generated by both algorithms was similar, with both selecting the same three parameters: ω_1, φ_1, and ER. Addition of calibration features (P_{min} or P_{max}) led to enhanced performance in the IF-ML models (*Table 2*).

Machine learning-based detection models for acute myocardial ischaemia

The best optimal classifiers for acute myocardial ischaemia (brief ischaemia without infarction) detection were selected based on similar accuracy threshold criteria to MI cases (see Supplementary material online, Supplement *B*). No trained model with uncalibrated input set passed our threshold criteria, so the selected IF-ML models for myocardial ischaemia detection are only for calibrated inputs including both ML techniques. *Table 3* demonstrates the characteristics and accuracy of selected models from RFC and SVC. ROC curves of the selected models for acute ischaemia detection are shown in *Figure 3*. Details about the optimal hyper-parameters of each classifier and the confusion matrices of the selected ischaemia models are provided in Supplementary material online, Supplement *E* (Supplementary material online, *Table S1*) and Supplement *F* (see Supplementary material online, Figure *S4*), respectively.

As shown in *Table 3*, the input vector $\{\omega_1, \varphi_1, P_{max}\}$ is the one picked by our selected optimal classifiers, so this input vector is the final suggestion of our physics-based feature selection for detection of acute myocardial ischaemia. Similar to acute MI, ω_1 and φ_1 were selected for ischaemia (coronary occlusion before infarction). This was expected since acute myocardial ischaemia and infarction have haemodynamic similarities.[9,12,29] In contrast to acute MI detection, both RF and SVC algorithms selected systolic pressure (P_{max}) instead of diastolic pressure (P_{min}) for ischaemia detection. Using a calibrated vector consisting of $\{\omega_1, \varphi_1, P_{max}\}$ as the input yielded the most accurate ML functions for detecting the occurrence of acute ischaemia (*Table 3*). Overall, the RFC performed slightly better for ischaemia detection. Particularly, the sensitivity for blind test data was higher for the RF-based model (sensitivity = 0.92) compared with the SVC model (sensitivity = 0.77). In terms of the AUC metric, the IF-ML model based on RF outperformed with a score of 0.95, compared with 0.82 for SVC. However, both classification techniques showed comparable specificity when tested on blind data (specificity = 0.85). Additionally, to validate our ML models against any possible overfitting, the 95% confidence intervals of all the models (whether MI or ischaemia detection) were obtained with multiple iterations of bootstrap resampling. The 95% confidence interval for AUC consistently fell within a safe range for all the selected models, with the widest range of ±0.07.

Discussion

Principal findings

Using a standard occlusion/reperfusion rat model,[31] we provided a preclinical proof-of-concept that a hybrid physics-based ML methodology, i.e. IF-ML, can detect the occurrence of acute MI or myocardial ischaemia (coronary occlusion before infarction) in rats from a single carotid waveform without using ECG. Since our approach was independent of ECG and pain, it can potentially be expanded in future clinical studies to facilitate detection of the so-called 'silent' (without chest pain) or 'super-silent' (without chest pain and ECG changes) MI. The results suggested that our IF-ML approach can accurately detect occurrence of an acute MI from an uncalibrated carotid waveform (best AUC = 0.94). Using calibrated pressure waveforms improved the performance of our approach (best AUC of 0.97). However, the IF-ML approach was able to accurately detect the occurrence of myocardial ischaemia (occlusion without infraction) from only calibrated carotid waveforms (best AUC = 0.95).

Diagnosis of myocardial infarction and ischaemia

Conventional methods for detection of acute MI or acute ischaemia are based on clinical criteria (e.g. pain) and ST segment change of ECG.[5] Although ECG is an important non-invasive and inexpensive test for diagnosis of acute MI and ischaemia, it requires expert interpretation. In addition, ECG is neither specific nor definitive[6] when used alone. Other advanced techniques/biomarkers for detection of MI or ischaemia (e.g. myocardial perfusion testing,[32] circulating BNP levels,[33] cardiac troponin levels,[34] or echocardiography[35]) have limitations such as invasiveness, radiation exposure, time to receive and analyse data, or cost. Here, we introduced a non-invasive approach for MI and ischaemia diagnosis that none of the above limitations is applicable to it. Although we have shown the invasive validation of our IF-ML methodology, numerous studies have validated non-invasive measurements of arterial pressure waveforms against invasively measured waveforms.[36,37]

Physics-based machine learning approaches in medicine

ML methodologies have recently become an emerging trend in medicine as they provide new perspectives for prognostics, diagnosis, and patient management. This is particularly evident in the realm of cardiovascular diseases, including conditions like hypertension, hypotension, and HF.[38–40] Due to their robustness, accuracy, and universality, ML

Table 2 Characteristics and accuracy summary of the selected optimal classifiers for acute myocardial infarction detection

Model	Input parameters	Training score	CV average score	Generalization accuracy	Blind test		All tests		All data	
					Spec	Sens	Spec	Sens	Spec	Sens
Uncalibrated RF	ω_1, φ_1, ER	0.96	0.70	0.86	0.85	0.85	0.86	0.84	0.91	0.91
Uncalibrated SVC	ω_1, φ_1, ER	0.72	0.72	0.79	1.00	0.85	0.90	0.84	0.80	0.78
Calibrated RF	ω_1, φ_1, ER, P_{min}	0.92	0.76	0.93	0.92	0.92	0.95	0.90	0.91	0.93
Calibrated SVC	ω_1, φ_1, ER, P_{min}	0.80	0.78	0.93	0.92	0.85	0.95	0.85	0.89	0.80

RF, random forest; SVC, support vector classifier; CV, cross-validation; Spec, specificity; Sens, sensitivity.

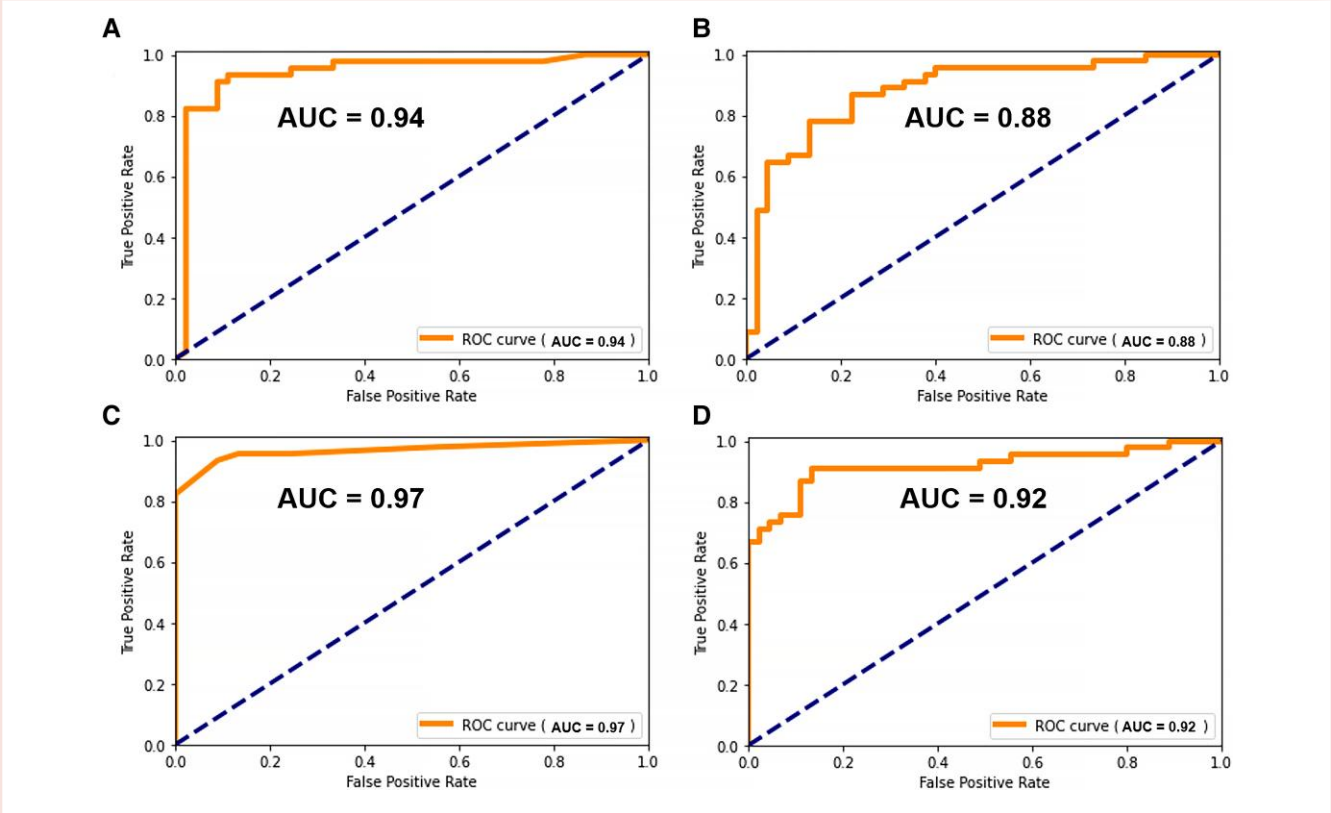

Figure 2 Receiver operating characteristic curve of the trained models for acute myocardial infarction detection using all data for (*A*) uncalibrated random forest, (*B*) uncalibrated SVC, (*C*) calibrated random forest, and (*D*) calibrated SVC models. Area under curve of each receiver operating characteristic curve is shown.

Table 3 Characteristics and accuracy summary of the selected optimal classifiers for acute myocardial ischaemia detection

Model	Input parameters	Training score	CV average score	Generalization accuracy	Blind test		All tests		All data	
					Spec	Sens	Spec	Sens	Spec	Sens
Calibrated RF	ω_1, φ_1, P_{max}	0.94	0.50	0.71	0.85	0.92	0.80	0.85	0.87	0.91
Calibrated SVC	ω_1, φ_1, P_{max}	0.74	0.66	0.86	0.85	0.77	0.85	0.80	0.82	0.73

RF, random forest; SVC, support vector classifier; CV, cross-validation; Spec, specificity; Sens, sensitivity.

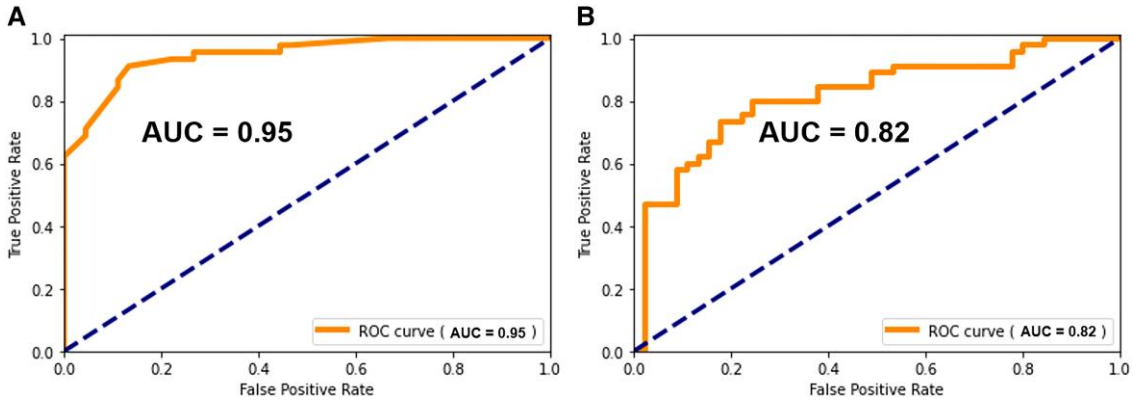

Figure 3 Receiver operating characteristic curve of the trained models for acute myocardial ischaemia detection using all data for (*A*) calibrated random forest and (*B*) calibrated SVC models. Area under curve of each receiver operating characteristic curve is shown.

models serve as powerful tools for early diagnosis and remote health monitoring.

Physics-informed (or physics-based) ML approximators, in particular, are very valuable to address problems of the cardiovascular system. Recently, hybrid physics-based ML methodologies that employ systems-level, reduced-order, or non-dimensionalized quantities have demonstrated promising results. They have been effective for assessing total arterial compliance or arterial pulse wave velocity, diagnosing and assessing the risk of coronary artery diseases, and evaluating cardiac contractility and aortic characteristic impedance[17,19,41–43]. In this study, we used the IF method to develop hybrid physics-based ML models. These models were designed to distinguish acute myocardial ischaemia or acute MI from normal healthy (baseline and non-occluded) conditions in rats using carotid pressure waveforms.

Intrinsic frequency-machine learning methodology for myocardial infarction/ischaemia detection

Acute coronary artery occlusion causes a sudden decrease in LV contractility and increase in LV end-diastolic pressure.[10,11,44] During the non-infarcted ischaemic period and infarcted period, cardiovascular system undergoes various regulatory responses that affect haemodynamics of the arterial system and LV-arterial coupling.[12,31] Based on the haemodynamic dependency of the IF parameters (a physics-informed approach),[14,15,18,21,25,45–48] we pre-selected ω_1, ω_2, φ_1, ER, and RHDN as inputs into our ML algorithms (see Methods section for details). Carotid systolic pressure (P_{max}) and diastolic pressure (P_{min}) were also included to consider calibrated pressure waveforms. Our results showed that ω_1, φ_1, and ER are the main determinants for detection of an acute MI. ω_1 strongly depends on the LV contractile performance,[15,21] and φ_1 is the intrinsic phase during the systole. The significance of these two parameters in acute MI is consistent with the haemodynamic alterations during coronary occlusion and acute MI.[11] ER represents the ratio of the energy stored in the systolic part of the pressure waveform over the diastolic portion, so it is mainly influenced by the dynamics of the arterial network (e.g. pulse wave velocity, total arterial compliance, peripheral resistance, etc.) and LV-arterial coupling.[17,21] The uncalibrated input vector of {ω_1, φ_1, ER} provided the most accurate IF-ML input vector for detection of the true class of acute MI occurrence since it covers haemodynamics changes associated with acute MI. The best calibrated models for MI detection (both SVC and RF) only picked P_{min} resulting in the input vector of {ω_1, φ_1, ER, P_{min}}, indicating that diastolic blood pressure provides supplementary information to IF parameters and improves the accuracy of acute MI detections.

Generally, the IF-ML approach performed better for MI detection compared with ischaemia detection in this study. This might be partly due to transient physiological variations caused by our experimental procedure during ischaemia. It may also be due to the higher haemodynamic complexity (e.g. mixed zone of myocardial cells in terms of functionality) of myocardial ischaemia compared with MI. We also ensured that our developed models did not just distinguish the baseline (healthy) from non-baseline (abnormal) events like post-occlusion events (see Supplementary material online, Supplement G). For example, we applied the calibrated-RF MI detection model on the ischaemic data (a different post-occlusion event than MI), and the predictions showed 55.6% MI vs. 44.4% no-MI, which shows the MI model predictions were not sensitive to myocardial ischaemia data points as another post-occlusion (abnormal) event. Moreover, our MI detection models more reliably detected severe infarctions characterized by larger infarct sizes (see Supplementary material online, Supplement *H* and Figure *S6* for the distribution of MI size over false and true positive predictions). As anticipated, false positive predictions were more associated with mild-to-moderate infarctions with smaller infarct sizes. More details can be found in Supplementary material online, Supplement *H*.

Strengths and limitations

The occlusion/reperfusion rat model used in this study is well established for recapitulating human pathophysiology and is close to clinical scenarios (see Lindsey *et al.*[31]) Our approach only requires pressure measurement without any need for ECG or flow/velocity measurements. The proposed hybrid approach relies on the IF method to capture the haemodynamic changes/signs of occurrence of MI or myocardial ischaemia and does not rely on the ML technique that is adopted. To show it, we applied two additional methods (i.e. artificial neural network and standard logistic regression) with the same design steps, and the developed models presented similar accuracies (see Supplementary material online, Supplement *I* and *Table S2*) as the other ML methods in the study (i.e. RF and SVC). Therefore, our proposed methodology works well no matter what ML approach is used. Although the present study is an invasive *in vivo* validation, all the required input parameters for our proposed ML models can be obtained non-invasively (e.g. using tonometry, Vivio, or a smartphone).[15,49]

While fully uncalibrated IF-ML models were our top priority, the proposed calibrated models (which use P_{min} or P_{max} i.e. diastolic/systolic pressures) still maintain the non-invasive and instantaneous advantage of the methodology. However, this comes at the cost of requiring calibrated pressure waveforms. One can easily obtain the calibrated waveform by knowing the values of systolic and diastolic blood pressures, which are sufficient for calibration. These values can also be measured non-invasively and remotely, for instance, using wearable cuff pressure devices. Thus, the developed calibrated IF-ML models would require cuff pressure measurements in conjunction with uncalibrated waveform measurement devices, such as an iPhone camera (see Pahlevan *et al.*[15]). Larger sizes of rat data for our ML methodology can lead to more confident models; however, this study serves as a promising proof-of-concept.

This study has limitations that should be considered. In this proof-of-concept study, we chose to use only female rats to maximize the survival rate of animals with confirmed infarction. Typically, in the standard 30-min occlusion/reperfusion rat model, male rats tend to experience more ventricular arrhythmias, which results in a higher mortality rate during the experiment compared with female rats. With the validation of the IF-ML methodology now established, future studies will also incorporate male rats. On the other hand, so far, our IF-ML methodology was developed and tested using only healthy rats at the baseline (before coronary occlusion). Using healthy rats (as the first step) was necessary to identify the true contributors for detection of acute MI or ischaemia. However, we acknowledge that future studies are needed to expand the methodology and confirm our IF-ML approach using older rats, spontaneously hypertensive rats, and rats that have undergone cardio-protective agents such as remote ischaemic pre-conditioning or hypothermia. Our current IF-ML models may underperform on such expanded and comprehensive databases that include rats with cardiovascular complications before coronary occlusion. Nevertheless, our study confirms that there exists an IF-ML model that can detect occurrence of acute MI or ischaemia that covers the full spectrum. We acknowledge the need for future pre-clinical and clinical studies to both confirm and broaden the applicability of the proposed IF-ML methodology. This includes its use in patients with hypertension, arterial stiffening, arrhythmia, as well as those with chronic ischaemic heart disease who receive common CVD prevention/treatment pharmacological therapies (e.g. beta-blockers, diuretics). In addition, in eventual clinical application, it would likely be more relevant to apply this method before the reperfusion in Catheterization labs, so a pre-reperfusion point might seem more clinically applicable for the MI point. However, in our 30-min occlusion/reperfusion rat model, we considered 2 h after reperfusion (which is also an MI point) for the MI. This decision was based on the understanding that, in this particular rat model, the infarction is well-developed after 2 h of reperfusion. This is mainly because the infarction process continues even after reperfusion, typically for 2 h, due to the phenomenon of 'Myocardial Reperfusion Injury'[50] (a myocardial injury resulting from the restoration of coronary blood flow after an ischaemic episode). Therefore, in our study using this rat model, the MI process is well developed at 2 h post-reperfusion, which we selected as the MI point. Additionally, during the short episode of 30-min occlusion in rats, the carotid waveforms are not particularly stable. However, they become stable a few hours after reperfusion. Another factor guiding our choice of 2-h post-reperfusion time point is the inability to measure the infarct size and quantify the degree of necrosis with just a 30-min coronary occlusion. At least a few hours of reperfusion are required to visualize the zone of necrosis using the TTC technique [which stains the lactate dehydrogenase (LDH) containing cells], as the LDH must wash out for visualization and confirmation of the infarction. The pre-reperfusion time point will be considered the MI point in our future clinical studies, which will investigate the translation of the methodology from pre-clinical to clinical stage.

Conclusions

This study presents the invasive validation of a physics-based hybrid IF-ML methodology for detection of the occurrence of acute MI or acute myocardial ischaemia from carotid pressure waveforms. We used invasively measured carotid pressure waveforms from a well-established coronary occlusion/reperfusion rat model to develop, validate, and blind-test our method. This study also provides the proof-of-concept that information about the occurrence of an acute MI or myocardial ischaemia can be extracted from carotid pressure waveforms. In its final form, our technique would require a small hand-held waveform recorder (e.g. smartphone-based devices or tonometer-type devices) or a wearable device, all of which could connect to a smartphone application.

Lead author biography

Rashid Alavi, MSc, is a PhD candidate in mechanical/cardiovascular engineering at Michelson center for convergent bioscience of University of Southern California (USC). He is currently working on his doctoral thesis entitled 'Hybrid Physics-based Data-driven Approaches for Noninvasive Hemodynamic Diagnosis of Myocardial Infarction and Heart Failure'. Rashid is part of several clinical and preclinical studies at USC Keck hospital and Huntington Medical Research Institutes (HMRI). Recently, Rashid has been nominated for the 2023 Young Investigator Award of the American College of Cardiology (ACC) as one of the top five finalists, competing with early career assistant professors, young cardiologists, postdocs, and cardiology fellows.

Data availability

The basic characterization data from the rats, which were used as a basis for the ML model designs and blind test, are presented in Supplementary material online, Supplement *J*. Any other data underlying this article will be shared on reasonable request to the corresponding author.

Supplementary material

Supplementary material is available at *European Heart Journal Open* online.

Funding

NMP is supported by the American Heart Association (AHA) Career Development Award No. 20CDA35260167.

Conflict of interest: NMP holds equity in Avicena LLC and has consulting agreement with Avicena LLC. Other authors have reported that they have no relationships relevant to the contents of this paper to disclose.

References

1. Benjamin EJ, Blaha MJ, Chiuve SE, Cushman M, Das SR, Deo R, de Ferranti SD, Floyd J, Fornage M, Gillespie C. Heart disease and stroke statistics—2017 update: a report from the American heart association. *Circulation* 2017:e146–e603.
2. Members WG, Roger VL, Go AS, Lloyd-Jones DM, Benjamin EJ, Berry JD, Borden WB, Bravata DM, Dai S, Ford ES. Executive summary: heart disease and stroke statistics—2012 update: a report from the American heart association. *Circulation* 2012;**125**: 188–197.

3. Braunwald E. Reduction of myocardial-infarct size. *New England Journal of Medicine* 1974;**291**:525–526.
4. Cannon CP, Gibson CM, Lambrew CT, Shoultz DA, Levy D, French WJ, Gore JM, Weaver WD, Rogers WJ, Tiefenbrunn AJ. Relationship of symptom-onset-to-balloon time and door-to-balloon time with mortality in patients undergoing angioplasty for acute myocardial infarction. *JAMA* 2000;**283**:2941–2947.
5. Maseri A. Pathogenetic mechanisms of angina pectoris: expanding views. *Br Heart J* 1980; **43**:648–660.
6. Khan MG. *Heart disease diagnosis and therapy: a practical approach*: Springer Science & Business Media; 2005.
7. Stephens JFIII. *The diagnostic value of a frequency analysis of the isovolumic contraction phase of the first heart sound*: University of Cincinnati; 1969.
8. Hershberg P. First aid therapy: a new concept in the treatment of myocardial infarction. *Med Times* 1968;**96**:575–591.
9. McCain FH, Kline EM, Gilson JS. A clinical study of 281 autopsy reports on patients with myocardial infarction. *Am Heart J* 1950;**39**:263–272.
10. Distante A, Picano E, Moscarelli E, Palombo C, Benassi A, L'abbate A. Echocardiographic versus hemodynamic monitoring during attacks of variant angina pectoris. *Am J Cardiol* 1985;**55**:1319–1322.
11. Sigwart U, Grbic M, Payot M, Goy J-J, Essinger A, Fischer A. Ischemic events during coronary artery balloon obstruction (ed.), *Silent myocardial ischemia*: Springer; 1984. p29–36.
12. Bristow JD, Arai AE, Anselone CG, Pantely GA. Response to myocardial ischemia as a regulated process. *Circulation* 1991;**84**:2580–2587.
13. Alavi R, Dai W, Amlani F, Rinderknecht DG, Kloner RA, Pahlevan NM. Scalability of cardiovascular intrinsic frequencies: validations in preclinical models and non-invasive clinical studies. *Life Sci* 2021;**284**:119880.
14. Cooper LL, Rong J, Pahlevan NM, Rinderknecht DG, Benjamin EJ, Hamburg NM, Vasan RS, Larson MG, Gharib M, Mitchell GF. Intrinsic frequencies of carotid pressure waveforms predict heart failure events: the Framingham heart study. *Hypertension* 2021;**77**: 338–346.
15. Pahlevan NM, Rinderknecht DG, Tavallali P, Razavi M, Tran TT, Fong MW, Kloner RA, Csete M, Gharib M. Noninvasive iphone measurement of left ventricular ejection fraction using intrinsic frequency methodology. *Crit Care Med* 2017;**45**:1115–1120.
16. Armenian SH, Rinderknecht D, Au K, Lindenfeld L, Mills G, Siyahian A, Herrera C, Wilson KD, Venkataraman K, Mascarenhas K, Tavallali P, Razavi M, Pahlevan N, Detterich J, Bhatia S, Gharib M. Accuracy of a novel handheld wireless platform for detection of cardiac dysfunction in anthracycline-exposed survivors of childhood cancer. *Clin Cancer Res* 2018;**24**:3119–3125.
17. Tavallali P, Razavi M, Pahlevan NM. Artificial intelligence estimation of carotid-femoral pulse wave velocity using carotid waveform. *Sci Rep* 2018;**8**:1014.
18. Mogadam E, Shavelle DM, Giesler GM, Economides C, Lidia SP, Duquette S, Matthews RV, Pahlevan NM. Intrinsic frequency method for instantaneous assessment of left ventricular-arterial coupling after transcatheter aortic valve replacement. *Physiol Meas* 2020;**41**:085002.
19. Alavi R, Dai W, Kloner RA, Pahlevan NM. A hybrid artificial intelligence-intrinsic frequency method for instantaneous detection of acute myocardial infarction. *Circulation* 2019;**140**:A12573–A12573.
20. Dai W, Amoedo ND, Perry J, Le Grand B, Boucard A, Carreno J, Zhao L, Brown DA, Rossignol R, Kloner RA. Effects of OP2113 on myocardial infarct size and No reflow in a rat myocardial ischemia/reperfusion model. *Cardiovasc Drugs Ther* 2022;**36**:217–227.
21. Pahlevan NM, Tavallali P, Rinderknecht DG, Petrasek D, Matthews RV, Hou TY, Gharib M. Intrinsic frequency for a systems approach to haemodynamic waveform analysis with clinical applications. *J R Soc Interface* 2014;**11**:20140617.
22. Alavi R, Wang Q, Gorji H, Pahlevan NM. Sequentially-reduced representation of artificial neural network to determine cardiovascular intrinsic frequencies. *bioRxiv* 2022; 2022.2002. 2014.480311. https://doi.org/10.1101/2022.02.14.480311
23. Hou TY, Shi Z. Adaptive data analysis via sparse time-frequency representation. *Adv Adapt Data Anal* 2011;**3**:1–28.
24. Aghilinejad A, Alavi R, Rogers B, Amlani F, Pahlevan NM. Effects of vessel wall mechanics on non-invasive evaluation of cardiovascular intrinsic frequencies. *J Biomech* 2021;**129**: 110852.
25. Petrasek D, Pahlevan NM, Tavallali P, Rinderknecht DG, Gharib M. Intrinsic frequency and the single wave biopsy: implications for insulin resistance. *J Diabetes Sci Technol* 2015;**9**:1246–1252.
26. Alavi R, Dai W, Arechavala RJ, Kleinman MT, Kloner RA, Pahlevan NM. Detection of the effect of nicotine delivered by E-cigarettes or standard cigarettes on cardiovascular system from a carotid waveform using a physics-based machine learning approach. *Circulation* 2022;**146**:A12922–A12922.
27. Alavi R, Dai W, Arechavala RJ, Kleinman MT, Kloner RA, Pahlevan NM. Nicotine delivered by electronic cigarette vapor or standard cigarettes adversely affects left ventricular systolic function measured by cardiovascular intrinsic frequency in rats. *Circulation* 2021;**144**:A13745–A13745.
28. Niroumandi S, Alavi R, Wolfson AM, Vaidya AS, Pahlevan NM. Assessment of aortic characteristic impedance and arterial compliance from non-invasive carotid pressure waveform in the Framingham heart study. *Am J Cardiol* 2023;**204**:195–199.
29. Kloner RA, Fishbein MC, Hare CM, Maroko PR. Early ischemic ultrastructural and histochemical alterations in the myocardium of the rat following coronary artery occlusion. *Exp Mol Pathol* 1979;**30**:129–143.
30. Abadi M, Agarwal A, Barham P, Brevdo E, Chen Z, Citro C, Corrado GS, Davis A, Dean J, Devin M. Tensorflow: large-scale machine learning on heterogeneous distributed systems. *arXiv preprint arXiv:160304467* 2016. https://doi.org/10.48550/arXiv.1603.04467
31. Lindsey ML, Bolli R, Canty Jr JM, Du X-J, Frangogiannis NG, Frantz S, Gourdie RG, Holmes JW, Jones SP, Kloner RA. Guidelines for experimental models of myocardial ischemia and infarction. *Am J Physiol Heart Circ Physiol* 2018;**314**:H812–H838.
32. Hachamovitch R, Berman DS, Shaw LJ, Kiat H, Cohen I, Cabico JA, Friedman J, Diamond GA. Incremental prognostic value of myocardial perfusion single photon emission computed tomography for the prediction of cardiac death: differential stratification for risk of cardiac death and myocardial infarction. *Circulation* 1998;**97**:535–543.
33. Sabatine MS, Morrow DA, De Lemos JA, Omland T, Desai MY, Tanasijevic M, Hall C, McCabe CH, Braunwald E. Acute changes in circulating natriuretic peptide levels in relation to myocardial ischemia. *J Am Coll Cardiol* 2004;**44**:1988–1995.
34. Ohman EM, Armstrong PW, Christenson RH, Granger CB, Katus HA, Hamm CW, O'Hanesian MA, Wagner GS, Kleiman NS, Harrell Jr FE. Cardiac troponin T levels for risk stratification in acute myocardial ischemia. *N Engl J Med* 1996;**335**:1333–1342.
35. Leischik R, Dworrak B, Sanchis-Gomar F, Lucia A, Buck T, Erbel R. Echocardiographic assessment of myocardial ischemia. *Ann Transl Med* 2016;**4**:259–259.
36. Kelly R. Non-invasive registration of the arterial pulse waveform using high fidelity applanation tonometry. *J Vasc Med Biol* 1989;**1**:142–149.
37. Salvi P, Lio G, Labat C, Ricci E, Pannier B, Benetos A. Validation of a new non-invasive portable tonometer for determining arterial pressure wave and pulse wave velocity: the PulsePen device. *J Hypertens* 2004;**22**:2285–2293.
38. Frizzell JD, Liang L, Schulte PJ, Yancy CW, Heidenreich PA, Hernandez AF, Bhatt DL, Fonarow GC, Laskey WK. Prediction of 30-day all-cause readmissions in patients hospitalized for heart failure: comparison of machine learning and other statistical approaches. *JAMA Cardiol* 2017;**2**:204–209.
39. Ahmad T, Lund LH, Rao P, Ghosh R, Warier P, Vaccaro B, Dahlström U, O'Connor CM, Felker GM, Desai NR. Machine learning methods improve prognostication, identify clinically distinct phenotypes, and detect heterogeneity in response to therapy in a large cohort of heart failure patients. *J Am Heart Assoc* 2018;**7**:e008081.
40. Hatib F, Jian Z, Buddi S, Lee C, Settels J, Sibert K, Rinehart J, Cannesson M. Machine-learning algorithm to predict hypotension based on high-fidelity arterial pressure waveform analysis. *Anesthesiology* 2018;**129**:663–674.
41. Bikia V, Rovas G, Pagoulatou S, Stergiopulos N. Determination of aortic characteristic impedance and total arterial compliance from regional pulse wave velocities using machine learning: an in-silico study. *Front Bioeng Biotechnol* 2021;**9**:649866.
42. Bikia V, Papaioannou TG, Pagoulatou S, Rovas G, Oikonomou E, Siasos G, Tousoulis D, Stergiopulos N. Noninvasive estimation of aortic hemodynamics and cardiac contractility using machine learning. *Sci Rep* 2020;**10**:1–17.
43. Alavi R, Dai W, Kloner RA, Pahlevan NM. A hybrid artificial intelligence-intrinsic frequency method for instantaneous determination of myocardial infarct size. *Circulation* 2020;**142**:A15899–A15899.
44. Distante A, Rovai D, Picano E, Moscarelli E, Morales MA, Palombo C, L'Abbate A. Transient changes in left ventricular mechanics during attacks of prinzmetal angina: A two-dimensional echocardiographic study. *Am Heart J* 1984;**108**:440–446.
45. Alavi R, Dai W, Kloner RA, Pahlevan N. INSTANTANEOUS DETECTION OF MYOCARDIAL ISCHEMIA FROM A SINGLE CAROTID WAVEFORM USING A PHYSICS-BASED MACHINE LEARNING METHODOLOGY. *J Am Coll Cardiol* 2023; **81**:4012–4012.
46. Alavi R, Dai W, Kloner RA, Pahlevan NM. A physics-based machine learning approach for instantaneous classification of myocardial infarct size. *Circulation* 2021;**144**: A12098–A12098.
47. Pahlevan NM, Alavi R, Ramos M, Hindoyan A, Matthews RV. An artificial intelligence derived method for instantaneous detection of elevated left ventricular End diastolic pressure. *Circulation* 2020;**142**:A16334–A16334.
48. Alavi R, Liu J, Ramos M, Hindoyan A, Matthews RV, Pahlevan NM. A hybrid machine learning method for instantaneous classification of left ventricular filling pressure using femoral waveforms. *Circulation* 2021;**144**:A14086–A14086.
49. Alavi R, Aghilinejad A, Wei H, Niroumandi S, Wieman S, Pahlevan NM. A coupled atrioventricular-aortic setup for in-vitro hemodynamic study of the systemic circulation: design, fabrication, and physiological relevancy. *PLoS One* 2022;**17**:e0267765.
50. Yellon DM, Hausenloy DJ. Myocardial reperfusion injury. *N Engl J Med* 2007;**357**: 1121–1135.